RBAV Revista Brasileira de Aplicações de Vácuo
https://doi.org/10.17563/rbav.v44i1.1262
REVIEW ARTICLE

VACUUM PROCESSES USED FOR HEAT AND SURFACE TREATMENTS OF STEELS AND SPECIALTY ALLOYS

Carlos Eduardo Pinedo[1,*], André Paulo Tschiptschin[2]

1. Heat Tech Technology for Heat Treatment and Surface Engineering Ltd and HTS Technology for Coatings Ltd – Mogi das Cruzes (SP), Brazil.

2. Universidade de São Paulo – Escola Politécnica – Departamento de Engenharia Metalúrgica e de Materiais – São Paulo (SP), Brazil.

Corresponding author: pinedo@heattech.com.br

Section Editor: Mariana Fraga

Received: Oct. 29, 2025 **Approved:** Nov. 28, 2025

ABSTRACT

The heat treatment of steels and specialty alloys has evolved over the years to meet the need for efficient processes that achieve specific microstructures and properties with minimal surface quality degradation caused by chemical interactions between the metal surface and the heat treatment environment. As a result, vacuum heat treatment furnace technology has gained an important position in industrial processes, ensuring microstructural metallurgical quality and surface integrity, with greater dimensional and shape stability and less distortion. Taking into account the importance of heat treatment in microstructural conditioning to achieve properties in the volume of the component body to withstand in-service demands, it is important to consider that wear and corrosion are important factors controlling the end of life of components for a wide range of industrial applications. Recently, there has been a growing effort to solve wear and corrosion problems through the use of surface treatments.[1,2] Surface engineering has been the focus of significant academic and research and development activities, and is increasingly used in industry through special vacuum processes such as plasma nitriding and physical vapor deposition coatings. These processes are important production routes and are environmentally friendly according to the management systems required by the ISO 14000.[3]

KEYWORDS: Heat treatment, Nitriding, Coating.

PROCESSOS SOB VÁCUO USADOS PARA TRATAMENTOS TÉRMICOS E DE SUPERFÍCIE DE AÇOS E LIGAS ESPECIAIS

RESUMO

O tratamento térmico de aços e ligas especiais evoluiu ao longo dos anos para atender à necessidade de processos eficientes que alcancem microestruturas e propriedades específicas com degradação mínima da qualidade da superfície causada por interações químicas entre a superfície do metal e o ambiente de tratamento térmico. Como resultado, a tecnologia de fornos de tratamento térmico a vácuo conquistou uma posição importante nos processos industriais, garantindo qualidade metalúrgica microestrutural e integridade da superfície, com maior estabilidade dimensional e de forma, e menos distorção. Levando em consideração a importância do tratamento térmico no condicionamento microestrutural para alcançar propriedades no corpo dos componentes, para suportar as demandas em serviço, é importante considerar que o desgaste e a corrosão são fatores importantes que controlam o fim da vida útil dos componentes para uma ampla gama de aplicações industriais. Recentemente, tem havido um esforço crescente para resolver problemas de desgaste e corrosão por meio do uso de tratamentos de superfície[1,2]. A engenharia de superfície tem sido um foco significativo de pesquisa acadêmica e de pesquisa e desenvolvimento, e é cada vez mais utilizada na indústria por meio de processos especiais sob vácuo, como nitretação sob plasma e revestimentos PVD (*physical vapor deposition*). Esses processos são importantes rotas de produção e ecologicamente corretos de acordo com os sistemas de gestão exigidos pela norma ISO 14000[3].

PALAVRAS-CHAVE: Tratamento térmico, Nitretação, Revestimento.

VACUUM HEAT TREATMENT

The use of heat treatment processes in vacuum furnaces increased and diversified from the 1980s onward, gaining markets in the automotive, aerospace, oil and gas, and biomedical sectors. This is primarily due to the possibility of rapid cooling within the vacuum chamber by the flow of inert gas, predominantly nitrogen, replacing the need for cooling in an external oil tank. The precision and reproducibility arising from process automation have also played an important role, and, finally, high-pressure cooling technology increased the capacity from the initial 2 bar to the current 20 bar. The increase in cooling pressure capacity has made it possible for quenching treatments of medium-hardenability steels, structural steels, and the solubilization of stainless steels and specialty alloys. The main advantages of heat treatment in vacuum furnaces are:

Surface integrity, protecting against oxidation and decarburization. Figure 1 shows tool batches after vacuum quenching and tempering heat treatment.

Possibility of programming complex thermal cycles, with heating and cooling at controlled rates and preheating steps.

Cooling under gas pressure at variable rates, adapting the cooling rate to the hardenability of the steels in the load and controlling distortion.

Use of interrupted cooling during quenching, martempering close to 550 °C, to homogenize cross-section temperature and obtain a homogeneous martensitic microstructure during quenching, with respect to the surface and core. This is especially applicable for large dies and parts to achieve homogeneous microstructures through the cross-section, minimizing distortion and preventing cracks.

Figure 1: Tools after quenching and tempering in a vacuum furnace.
Source: Courtesy of Heat Tech Tecnologia em Tratamentos Térmicos e Engenharia de Superfície Ltda.

Regarding the dimensional stability of parts with complex shapes, the main advantage of gas-cooled quenching is the homogeneity of the temperature profile through the cross-section. Unlike liquid quenching, in which the cooling mechanism leads to heterogeneous heat extraction and a heterogeneous temperature profile across the quenched part, high-pressure gas quenching uses convective heat exchange as its fundamental mechanism, and the cross-section temperature profile is highly favorable for minimizing shape variation due to heterogeneous dimensional changes in different positions and sections of complex parts. Figure 2 shows the difference between the heat extraction rate and the temperature profile across the part for liquid and gas quenching, which is crucial for minimizing distortion.[4]

Gas quenching rates vary with the gas injection pressure. As shown in Fig. 3, the quenching rate increases with increasing nitrogen injection pressures from 1 to 5 bar.[5] Advances in vacuum furnace technology currently allow for the use of injection pressures up to 20 bar, enabling the quenching of a wide range of steels, from engineering steels, such as SAE 4140 and 4340, with lower hardenability, to high-alloy steels such as tool steels and MSS stainless steels, with high hardenability. It is important to point out that quenching gas pressure must satisfy only the hardenability limitation of steels, and the use of higher gas quenching pressures will increase the tendency to distortion.

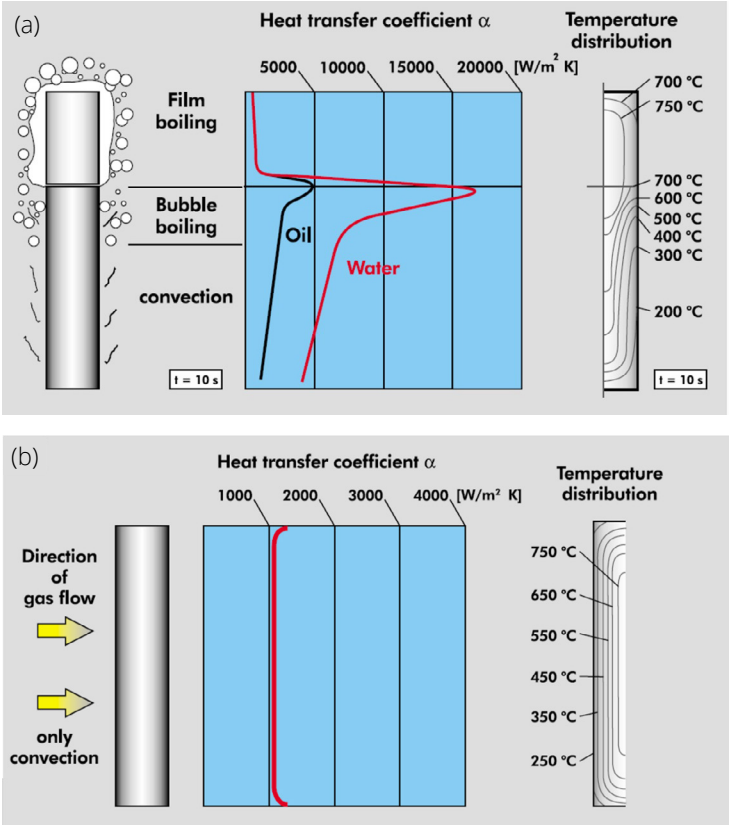

Figure 2: Schematic representation of heat exchange during cooling in liquid media, oil, and water (a), and with gas flow (b).[4]

Source: Adapted from Liščić.[4]

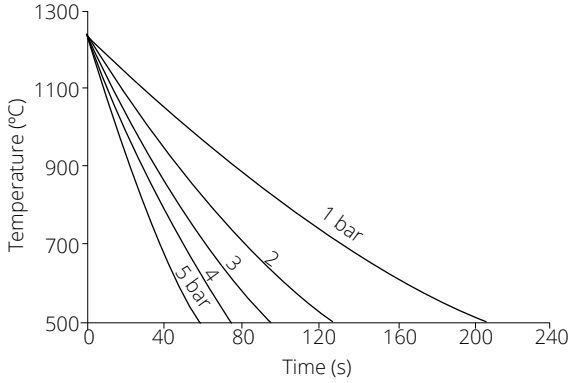

Figure 3: Cooling rates for different nitrogen injection pressures on quenching of 25.0 mm round bars of high-speed steel type AISI M2.[5]

Source: Adapted from Totten.[5]

Cooling efficiency also depends on the vacuum furnace's construction system. The gas must circulate inside the chamber and reach all parts as evenly as possible. Figure 4 illustrates a system with gas nozzles distributed diametrically throughout the furnace chamber (white arrows), from front to bottom, which allows for complete and homogeneous injection throughout the chamber volume. In this system, cold injected gas reaches the parts for cooling, heats up, and returns hot through the cooling system to become cold and continue the cooling process.

An important application of such a cooling system is when quenching hot work tool steels. During cooling from austenitizing temperature, precipitation of proeutectoid carbides is expected for low cooling rates. These proeutectoid carbides, as a network on previous austenite grain boundaries, are responsible for a decrease in fracture toughness and impair the performance of these steels, such as AISI H11 and AISI H13.[7]

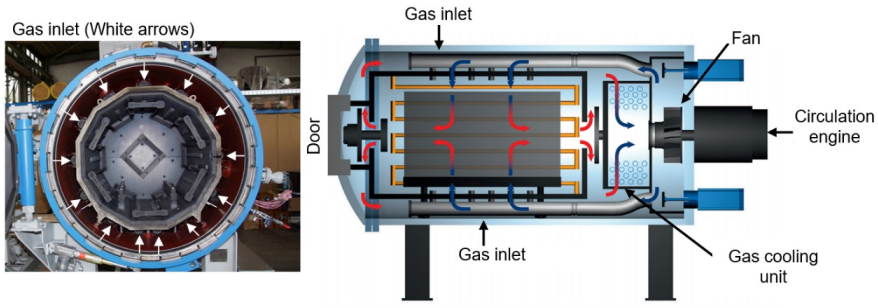

Figure 4: Vacuum furnace with indication of nitrogen inlets (white arrows), gas circulation, and cooling system.[6]
Source: Adapted from Ruffle and Byrnes.[6]

The North American Die Casting Association (NADCA), in collaboration with leading companies in the die casting industry, issued a standard with recommendations for heat treatment quality microstructure, NADCA #207-2003, to achieve the best fracture toughness. According to NADCA, the minimum cooling rate for these steels in gas pressure quenching in vacuum furnaces must be 27 °C/minute.[8] Figure 5 shows the microstructure of American Iron and Steel Institute (AISI) H11 hot work tool steel cooled to achieve acceptable NADCA quality compared to the unacceptable condition with grain boundaries marked by the precipitation of proeutectoid carbides.

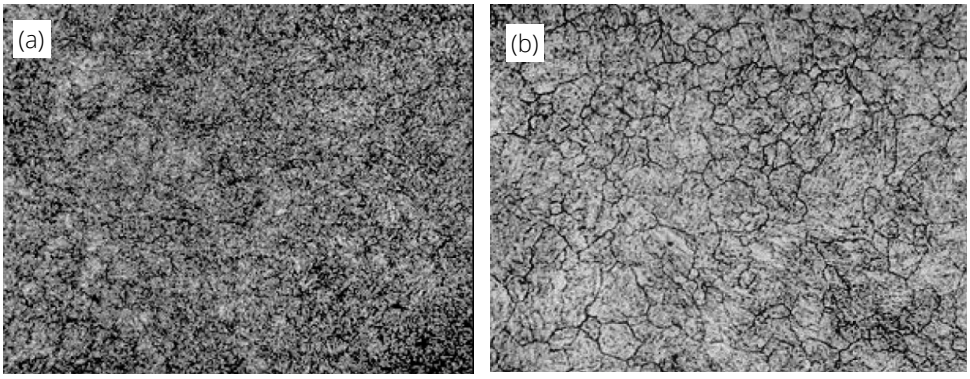

Figure 5: Comparison between the microstructural quality of AISI H11 steel cooled at different rates to achieve the quality after heat treatment specified by NADCA. Nital. 500x.[9]
Source: Adapted from Wingens.[9]

INTERSTITIAL DIFFUSION SURFACE HARDENING PROCESSES

Austenitic (ASS), MSS, duplex (DSS), and precipitation hardening (PH) stainless steels have been used in a variety of applications within the refining and petrochemical industry, where high corrosion resistance and mechanical properties are required. However, for many applications, the stainless steel hardness is not sufficient to withstand the tribological conditions of the system that cause wear, even for quenched and tempered MSS.[10]

Thermochemical and plasma-assisted treatments may improve the surface properties of these steels to reach better performance in highly stressed tribological systems. Different thermochemical and plasma-assisted surface processes have been proposed to improve the tribological properties of these corrosion-resistant alloys, such as high temperature gas nitriding (HTGN), low temperature gas carburizing (LTGC), low temperature plasma nitriding (LTPN), low temperature plasma carburizing (LTPC), and low temperature plasma nitrocarburizing (LTPNC).[11-13]

Surface treatments involving the diffusion of interstitial elements aim to diffuse nitrogen and/or carbon to form a supersaturated solid solution of the metallic matrix, thereby increasing surface hardness through the development

of compressive residual stresses on the surface. To preserve corrosion resistance, surface diffusion enrichment of chromium nitrides or chromium carbides precipitation at grain boundaries must be avoided, because such precipitation will generate a chromium-depleted zone that decreases corrosion resistance (sensitization phenomena), as shown in Fig. 6.[14,15]

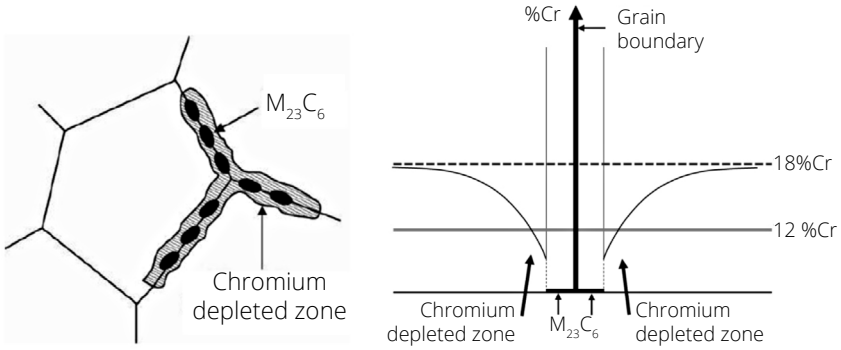

Figure 6: $Cr_{23}C_6$ precipitation harms the corrosion resistance due to Cr content depletion (sensitization).[14,15]
Source: Adapted from France and Greene.[14,15]

Surface treatments involving the diffusion of interstitial elements aim to diffuse nitrogen and/or carbon to form a supersaturated solid solution of the metallic matrix, thereby increasing surface hardness through the development of compressive residual stresses on the surface.

High Temperature Gas Nitriding

High Temperature Gas Nitriding (HTGN) makes it possible to obtain high equilibrium nitrogen contents, up to 1.1 wt.%, in solid solution in austenite, depending on SS chemical composition, N_2 potential in the nitriding atmosphere, nitriding temperature, and pressure, according to Fig. 7. It is a solid-state nitrogen alloying technique, consisting of exposing the SS to a high-purity N_2-containing gas atmosphere in the range 1,000-1,200 ºC. Atomic nitrogen is interstitially absorbed at the surface of the steel and then diffuses into the near-surface region, promoting hardening and improving corrosion resistance. Pitting corrosion resistance is significantly enhanced when high nitrogen contents are maintained in solution within the austenite, according to Fig. 8.

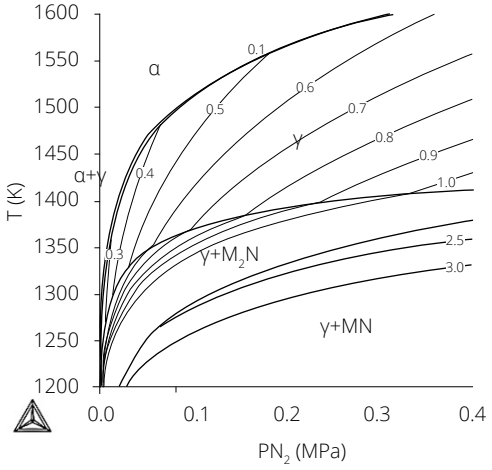

Figure 7: Phase fields and nitrogen iso-concentration lines for a Fe-16.2 wt.% Cr alloy.[16]
Source: Adapted from Garzon and Tshiptschin.[16]

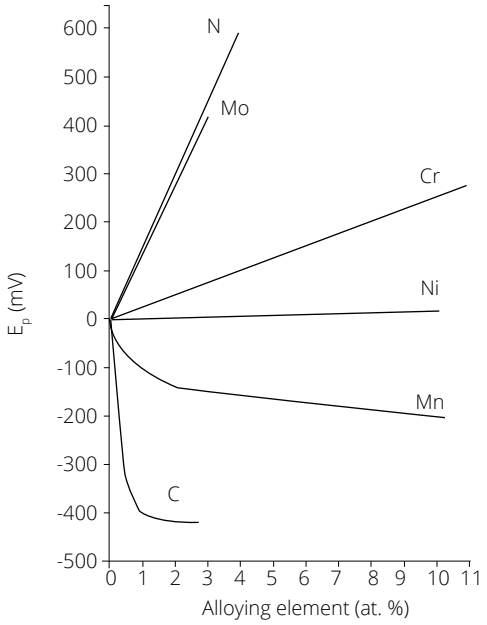

Figure 8: Change in pitting potential of 18 wt.% Cr ASS stainless steels in dilute chloride solution.[17]

Source: Adapted from Speidel.[17]

High-temperature gas nitriding can be performed on different types of stainless steels, obtaining case-hardening layers with various microstructures. When HTGN is carried out on a fully ASS nitrogen-rich surface layer is obtained. When HTGN is carried out on a high-hardness, fully ASS nitrogen-rich surface layer is obtained (Fig. 9). When HTGN is carried out on a dual-phase (γ + M), a fully nitrogen-rich MSS layer is obtained. When HTGN is carried out on a fully nitrogen-rich MSS layer is obtained. The stainless steels obtained through HTGN can be used in different applications, depending on the surface properties: a) high-hardness stainless steels (MSS cases) are used in roller bearings and tools; b) wear-resistant (high-nitrogen ASS cases) stainless steels, which are highly resistant to cavitation-erosion and erosion-corrosion, are used in pump rotors in slurry environments; c) corrosion-resistant stainless steels (generalized and localized corrosion) are used in surgical implants, biomedical applications, retaining rings, etc.

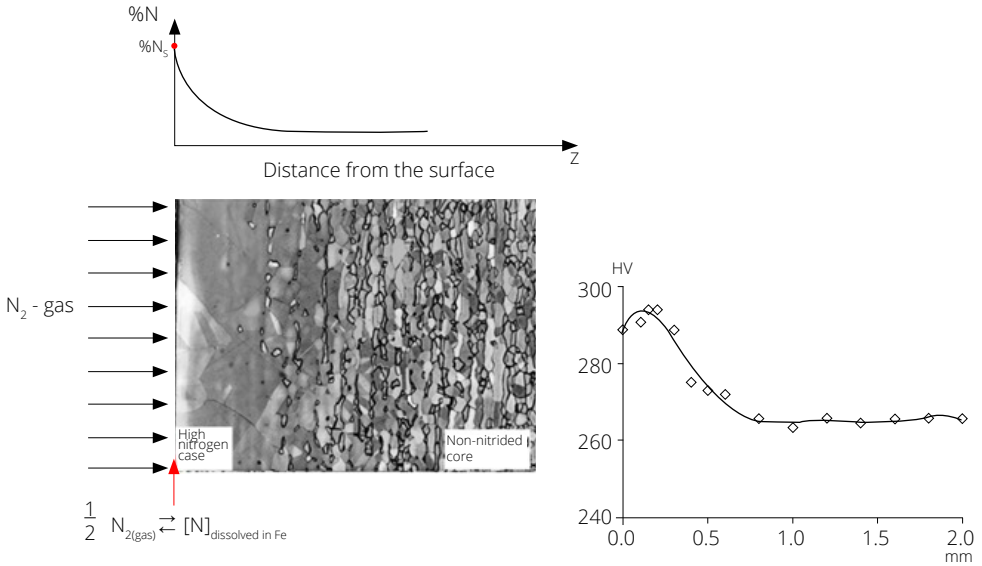

Figure 9: HTGN applied to DSS (α+γ) stainless steel, resulting in a thick, high-nitrogen, fully ASS case.[18]

Source: Adapted from Garzon and Tschiptschin.[18]

Before HTGN, the parts should be blasted with glass beads to remove the passive film mechanically. The heating-up should be carried out under vacuum, by mechanical pumping, to purge the furnace atmosphere and minimize oxygen partial pressure. Pure titanium scraps were used inside the chamber to trap and reduce the remaining oxygen. This procedure is essential because it is well known that residual oxygen impairs nitrogen diffusion due to the high oxidation kinetics of SS. According to previous work,[18] the optimum nitriding temperature for DSS is between 1,150 and 1,175 °C, and a high-temperature nitriding step was carried out at 1,150 °C for 12.5 hours. Figure 9 shows the fully ASS case microstructure of an HTGN-treated UNS 31803 DSS stainless steel. The high nitrogen case is hardened by the nitrogen atoms in solid solution to a depth of 0.5 mm. Figure 10 shows the partial nitrogen pressures used during the HTGN cycle.

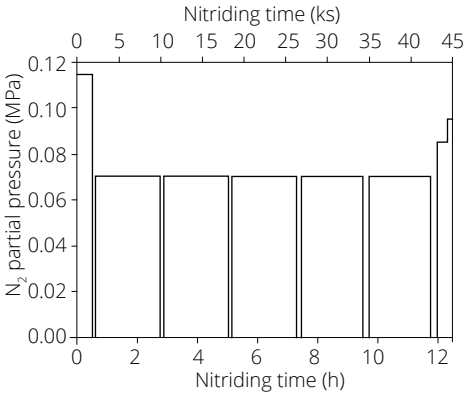

Figure 10: Nitrogen partial pressure as a function of nitriding time for the cyclic nitriding treatment.[18]
Source: Adapted from Garzon and Tschiptschin.[18]

To improve the surface hardness by high temperature interstitial hardening (HTIH), as HTGN, without loss of corrosion resistance, fast cooling must be employed to avoid precipitation of chromium-rich carbides, leading to sensitization, as "path A" shown in Fig. 11. For low temperature interstitial hardening (LTIH), Fig. 11 shows the maximum temperature at which processes can be carried out without precipitation of carbides.

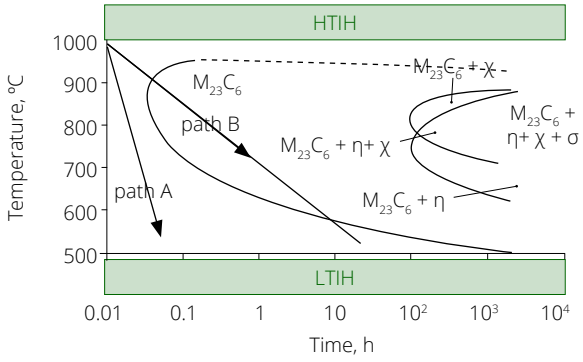

Figure 11: Cooling paths A and C avoid $Cr_{23}C_6$ precipitation, which harms the corrosion resistance.[19]
Source: Adapted from Collins et al.[19]

Low-temperature hardening of stainless steel

Through LTIH of stainless steels, one can improve the surface hardness without losing the corrosion resistance. The first low-temperature diffusion surface treatment for stainless steels was introduced by Kolster[20] and was named "Kolsterising," now a trademark of the Bodycoat company. Indeed, the interstitial expanded phase, called "S-Phase," or "Shifted Phase," was discovered by Ichii,[21] who named it due to the shift of the γ(111) peak in the X-ray diffraction pattern appearing shifted to the left due to the nitrogen supersaturation and expansion of the face-centered cubic lattice, as shown in Fig. 12.

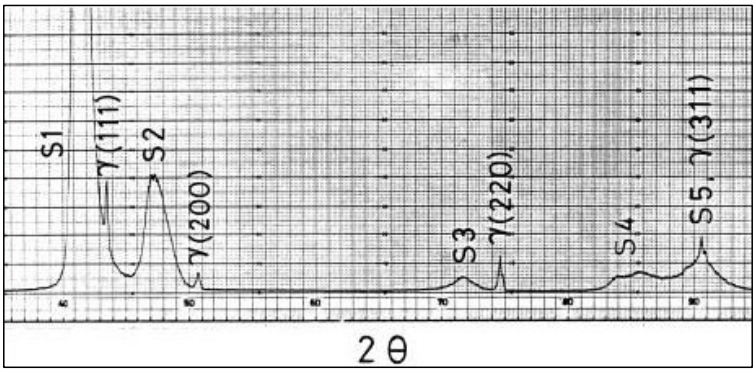

Figure 12: X-ray diffraction patterns of the "S-Phase" showing the formation of a metastable, precipitate-free, interstitial supersaturated, super-hard "expanded austenite" phase.[21]

Source: Adapted from Ichii et al.[21]

To perform carbon or nitrogen LTIH, it is necessary to perform a Surface Activation Treatment to remove the Cr_2O_3 passive layer. Three methods have been proposed:

- Depassivation by halide-containing atmospheres: NF_3 or HCl – LTGC (patent by Swagelok);
- Activation of the surface of the part with Ni metal to prevent repassivation through catalytic NH_3 gas decomposition (patent by Somers US 7431778 B2);
- Activation of the surface by DC/plasma sputtering in H_2, under a high applied voltage and low pressure – patent 018090023300 Instituto Nacional da Propriedade Industrial (INPI) by Tschiptschin and Pinedo.

LTIH makes it possible to obtain nitrogen, carbon, or nitrogen/carbon expanded phases. Figure 13 shows the formation of nitrogen expanded austenite (γ_N), obtained through "LTPN," carbon expanded austenite (γ_C), through "LTPN," and (γ_N+γ_C) expanded austenites through "LTPNC."[22] Such treatments producing "γ_N" and/or "γ_C" lead to different properties, as summarized in Table 1.[23] Figure 14 shows the transverse hardening profiles for expanded austenites obtained in Fig. 13, confirming the information from Table 1, such as maximum hardening and transverse hardening profile through the plasma-treated surface.

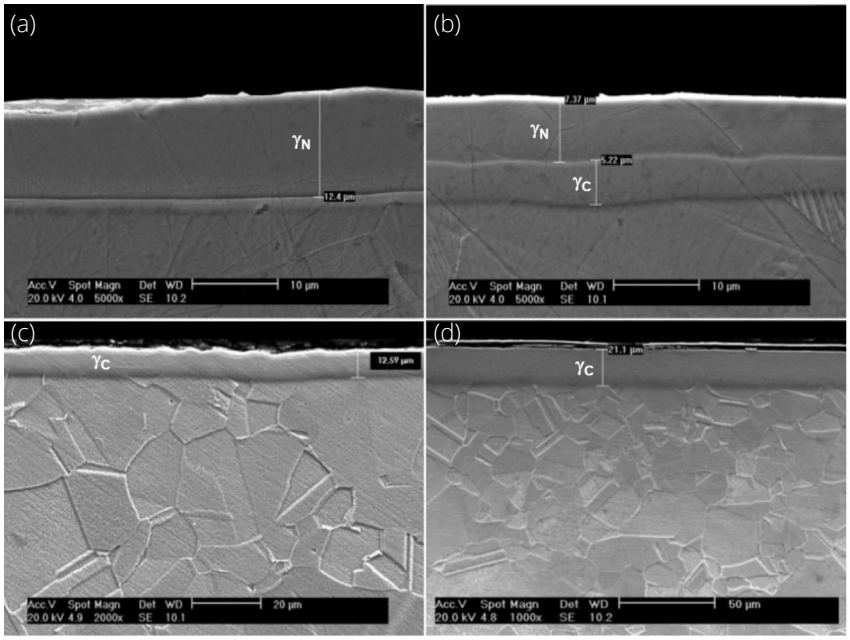

Figure 13: Formation of expanded phases: (a) nitrogen expanded austenite (γ_N) obtained after LTPN at 400 °C, (b) nitrogen expanded austenite (γ_N) and carbon expanded austenite (γ_C) obtained after LTPNC at 400 °C, (c) carbon expanded austenite (γ_C) obtained after LTPC at 400 °C, and (d) carbon expanded austenite (γ_C) obtained after LTPC at 480 °C.[22]

Source: Adapted from Pinedo and Tschiptschin.[22]

Table 1: Main characteristics of N-rich and C-rich S-phase[23]

Properties	N-rich "S-Phase" (γ_N)	C-rich "S-Phase" (γ_C)
Formation temperature (°C)	300-450	300-550
Maximum interstitial content (at. %)	38	19
Maximum surface hardness (HV)	1,450	1,000
Hardness profile	Abrupt	Gradual
Toughness	Poor	Good
Load-bearing capacity	Low	High
Dry sliding wear resistance	Very good	Good
Localized corrosion resistance	Very good	Good
Threshold temperature decomposition (°C)	350	300

Source: Adapted from Borgioli.[23]

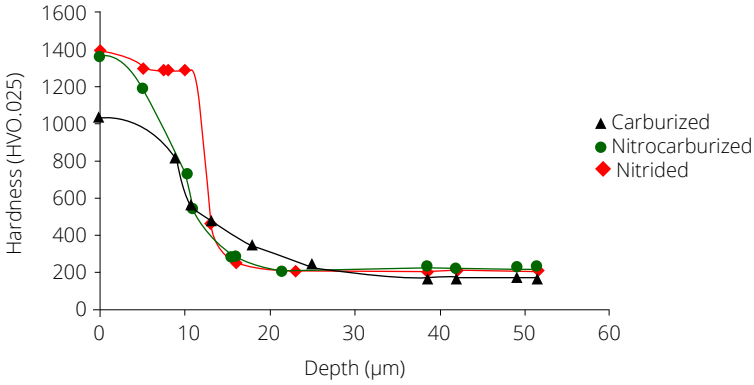

Figure 14: Hardness profiles of the 400 °C LTPN, 400 °C LTPNC, and the 480 °C LTPC surface-treated specimens.[22]
Source: Adapted from Pinedo and Tschiptschin.[22]

Berghaus conceived the plasma nitriding process in the early 1930s, but it was not disseminated industrially due to difficulties in controlling the main physical parameters of the process at that time.[24-26] With technological advances in logic control, programming, and automation systems, plasma nitriding gained prominence in industry. Nowadays, plasma nitriding is a technology increasingly used worldwide, particularly in Brazil. Among the industrially available nitriding processes, plasma nitriding stands out for its versatility, precision, and reproducibility in controlling the microstructure and properties of the nitrided surface, as well as being a non-pollutant process.[27] In specialty steels and alloys, control of the main process parameters such as temperature, time, and gas mixture composition, as well as the response of the substrates with different chemical compositions, is the key knowledge to generate distinct nitride surfaces with controlled properties, particularly in terms of surface hardening capacity and corrosion resistance.

The principle of the plasma nitriding process consists of producing nascent nitrogen by accelerating electrons through an electric field to give them enough energy to cause the decomposition of the gas and the generation of positively charged ions, as per the reaction in equation 1.[28] The ionized nitrogen, together with the electrons, forms a mixture with a very close ratio of positive to negative charges. These particles form the plasma:

$$e^- \rightarrow N_2 = N^+ + N^+ + 2e^- \quad (1)$$

The schematic of a hot-wall plasma nitriding furnace is shown in Figure 15. The process uses a pulsed DC voltage source that generates a potential difference between the anode (+), which corresponds to the furnace bell, and

the cathode (-), which corresponds to the parts being treated. Process gases are introduced into the chamber by a central unit equipped with high-precision mass flow meters, which generate gas mixtures in proportions defined for each process. A vacuum pump, coupled to a flow valve, controls the chamber's internal pressure. The process temperature is controlled by thermocouples that can be positioned directly on the parts or on coupons of equivalent mass. The plasma nitriding furnace uses high-purity nitrogen, hydrogen, argon, and methane, analytical grade 5.0, as process gases. These gases are injected in specific mixtures and quantities that depend on the structure of the nitrided surface that is desired and the type of steel being nitride.[29-31]

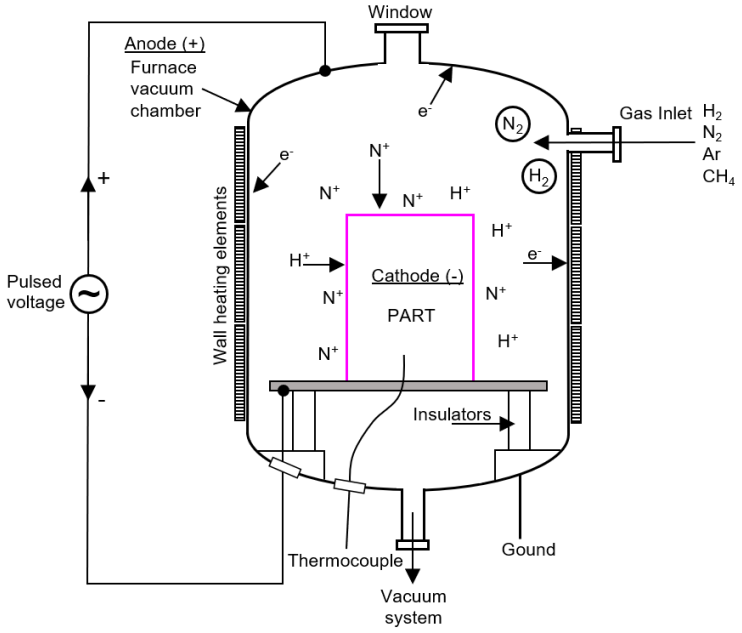

Figure 15: Diagram of a plasma nitriding reactor.[29]
Source: Adapted from Pinedo.[29]

The correct combination of temperature, pressure, voltage, and gas composition allows for a sustainable and homogeneous plasma for the process. The main advantage of the plasma nitriding process is the possibility of controlling the microstructure of the nitrided surface through precise control of the composition of the process gas mixture. Precise control of the nitrogen potential in the atmosphere allows for the modification of the surface microstructure to obtain a white layer composed predominantly of γ'(Fe_4N) or ε($Fe_{2-3}N$) nitrides, or even without a white layer, as shown in Fig. 16.

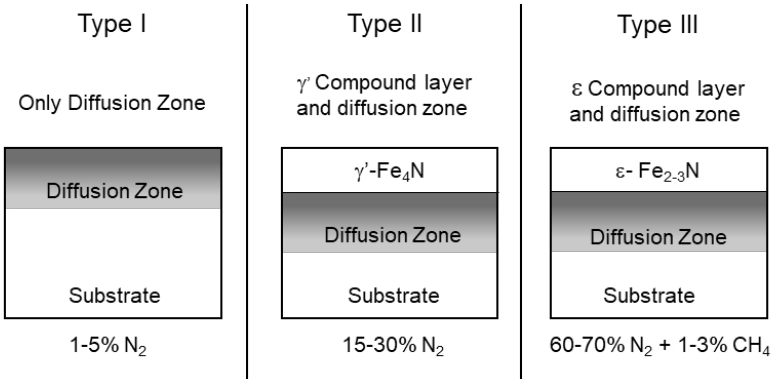

Figure 16: Possibilities of modifying the microstructure of the NC depending on the composition of the gas mixture in the atmosphere.[32,33]
Source: Adapted from Spalvis.32 and Elwart and Hunger.[33]

Although plasma nitriding can precisely control the composition of the gas mixture over a wide range of nitrogen potentials, for process efficiency, it is essential to generate a plasma with sufficient intensity and consistency. The presence of a plasma is responsible for generating the active ionic species in the nitriding process: the nitrogen ion. The principle of the plasma nitriding process consists of producing nascent nitrogen by accelerating electrons through an electric field to give them enough energy to cause the decomposition of the gas and the generation of positively charged ions.[34]

Figure 17 shows the relationship between voltage and current density, their different effects, and the region of formation of the abnormal glow that generates a "glow discharge," corresponding to the combination of voltage and current density to generate a stable and homogeneous "plasma sheath" around the parts' surface for the nitriding process.[33] Figure 18 shows that the glow discharge is formed homogeneously involving each piece of the load, which makes it possible to obtain a nitrided case (NC) with a microstructure and properties that are reproducible in all pieces of the batch.

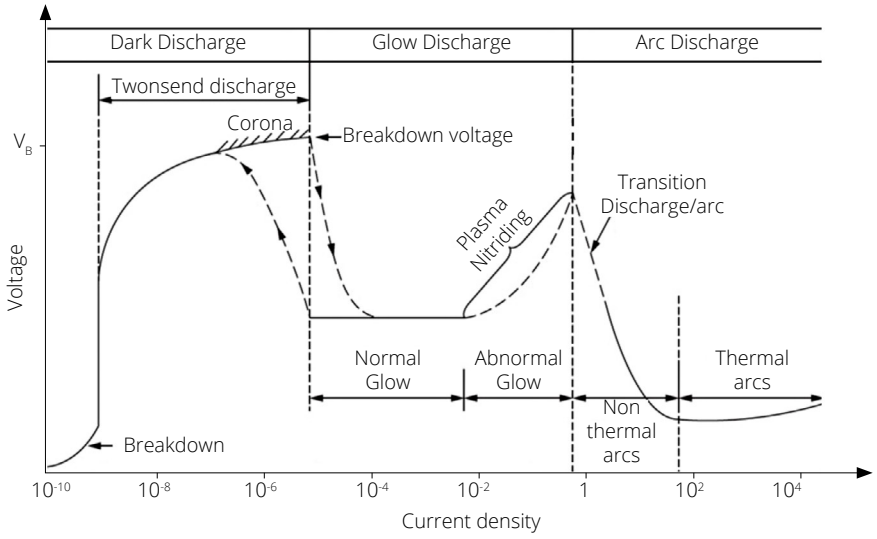

Figure 17: Relationship between voltage and current for the generation of the abnormal discharge or "glow discharge," corresponding to the plasma nitriding regime.[33]

Source: Adapted from Elwart and Hunger.[33]

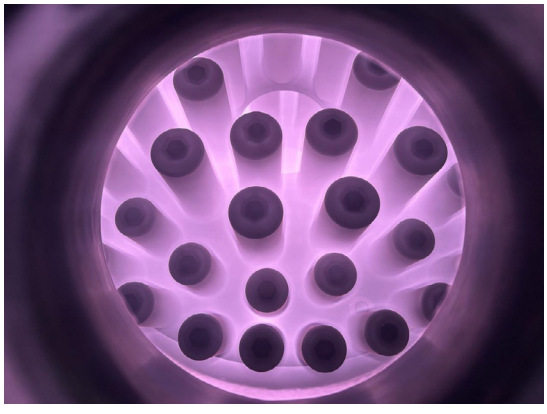

Figure 18: Glow discharge covering parts manufactured from AISI 316 ASS stainless steel during the plasma nitriding process.

Source: Courtesy of Heat Tech Tecnologia em Tratamentos Térmicos e Engenharia de Superfície Ltda.

It is important to point out that the ability to obtain and maintain a sustainable and active plasma depends on fundamental process parameters such as pressure and distance between the electrodes, which control the breakdown voltage V_b. However, the gas mixture also modifies the process conditions for obtaining a minimum

V_b value, which is particularly important considering that the composition of the gas mixture H_2:N_2 is responsible for controlling the microstructure of the nitrided layer, as shown in Figure 16. The electrical characteristics of the H_2:N_2 mixture glow discharge for different process conditions in plasma nitriding pure iron are shown in Fig. 19 at a constant distance between the two electrodes of 1.5 cm. The breakdown voltage (V_b) is a function of H_2 content in the H_2:N_2 gas mixture at different process pressures.[35]

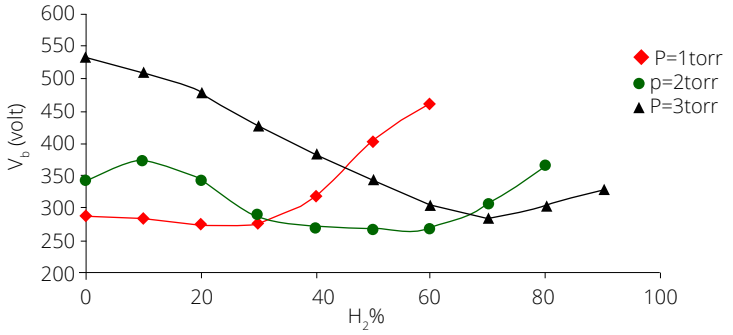

Figure 19: Breakdown voltage (V_b) for different pressure conditions of the plasma nitriding process as a function of H_2 content in the N_2:H_2. d = 1.5 cm.[35]
Source: Adapted from Elwart and Hunger.[33]

Nowadays, plasma nitriding furnaces have software and PLC systems capable of controlling the main process variables to maintain a homogeneous, active, and efficient plasma for safe nitriding within the design originally proposed for the load. Figure 20a shows a photograph of a nitriding charge seen from the furnace window. The presence of the stable and homogeneous plasma around the part and inside the holes is clearly observed. One of the parts nitrided during the process of Fig. 20a is shown in Fig. 20b and characteristically presents an opaque gray color, corresponding to the presence of the white layer that is homogeneous across the surface and within the holes.

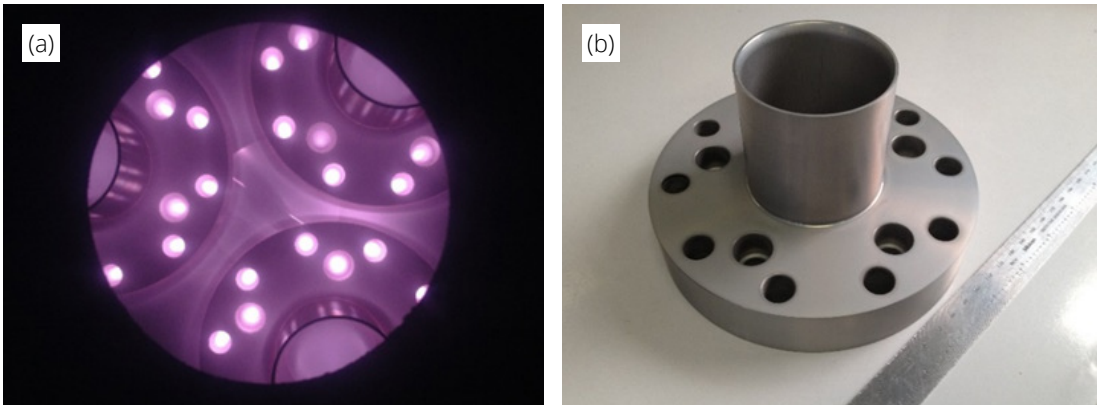

Figure 20: View of parts in a plasma nitriding load from the furnace window (a) and a part after the plasma nitriding process (b).
Source: Courtesy of Heat Tech Tecnologia em Tratamentos Térmicos e Engenharia de Superfície Ltda.

The superior corrosion resistance and high-temperature properties of Inconel 625 make this alloy an important choice in critical parts for oil and gas, nuclear, aerospace, and other sectors.[36,37] For some critical applications, however, optimization of its surface properties is needed to optimize its tribological behavior, increasing wear resistance. In these cases, the diffusion of interstitial elements in the solid state, such as LTPN, has proven to be an alternative for improving wear resistance by increasing surface hardness without compromising corrosion resistance.[37] As in other austenitic matrix alloys, the diffusion of nitrogen and/or carbon leads to the formation of expanded austenite.[37-40]

Important results on LTPN surface treatment for Inconel 625 superalloy are summarized in this review. Detailed experimental procedures were previously published by Varela et al.[41] Plasma nitriding treatment was carried out in a DC hot-wall plasma nitriding furnace at 420 °C for 20 hours with a gas mixture of 75%N_2:25%H_2, under 250 Pa pressure. Figure 21 shows the NC composed of expanded austenite (γ_N) with a thickness of 8.36 ± 0.13 µm.

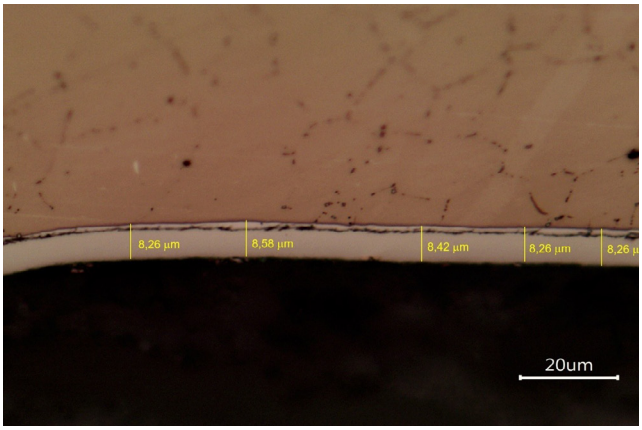

Figure 21: Optical micrograph of the NC of Inconel 625 superalloy, electrolytically etched with 10% oxalic acid.[41]
Source: Adapted from Varela et al. [41]

The surface enrichment in the interstitial element nitrogen through the cross-section obtained in the plasma nitriding of the Inconel 625 alloy is shown in Fig. 22. The general nitrogen diffusion profile is diffuse, with a gradual decrease in concentration towards the core, typical of low-temperature plasma treatments. The diffusion depth is approximately 6.0 µm, corresponding to the expanded austenite region observed by scanning electron microscopy.

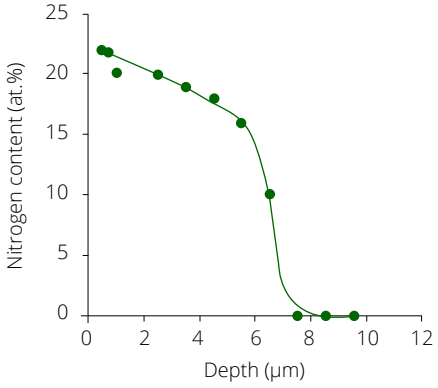

Figure 22: Nitrogen depth concentration of expanded austenite case after LTPN Inconel 625.[41]
Source: Adapted from Varela et al.[41]

The variation in surface hardness, determined by Vickers microhardness, as shown in Fig. 23, follows the diffuse behavior of the nitrogen compositional profile. Hardness is highest near the outermost surface and gradually decreases towards the core. The maximum measured hardness was 930 HV0.01, three times higher than the initial hardness of the solution-treated, non-nitrided alloy, which was 285 HV0.01.

The improvement in wear resistance is evident after microabrasion wear testing. Figure 24 compares the results in the solution-treated and plasma-nitrided conditions at 420°C, showing a smaller volume worn during the test after nitriding. The formation of expanded austenite after nitriding (γ_N = 939 HV) is responsible for the improvement in wear resistance compared to the initial state of the solution-treated matrix (γ = 285 HV). As a result, the wear coefficient decreases from 1.1 × 10^{-4} mm³/mN in the non-nitrided condition to 4.1 × 10^{-5} mm³/mN after nitriding.

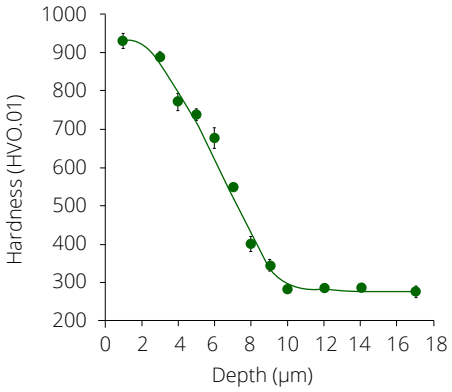

Figure 23: Transverse microhardness profile of the NC after LTPN in Inconel 625.[41]
Source: Adapted from Varela et al.[41]

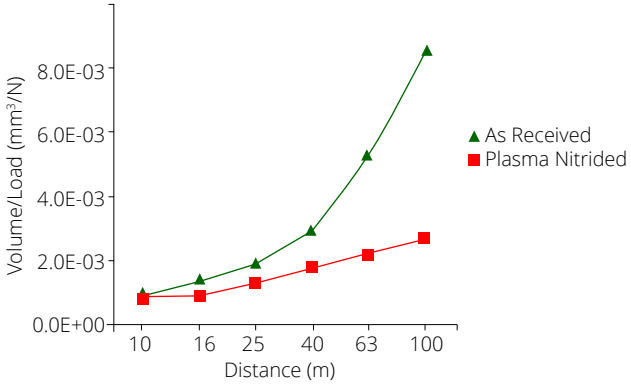

Figure 24: Volume loss per load unit as a function of the distance of plasma nitrided Inconel 625 and as-received non-nitrided samples.[41]
Source: Adapted from Varela et al.[41]

PHYSICAL VAPOR DEPOSITION (PVD) COATING

Different from nitriding processes, which involve the diffusion of the interstitial element nitrogen into the steel's crystal lattice, promoting surface enrichment and surface hardening, PVD coatings have high hardness, low coefficient of friction, with very high wear resistance compared to bulk. The layer, so-called "film" or "coating," is composed of a metallic fraction, such as Ti, Cr, Al, etc., or alloys of TiAl, CrAl, etc., and a non-metallic fraction containing nitrogen and/or carbon. These films are then called "nitrides," "carbonitrides," or "carbides." Each type of film has specific properties: hardness, coefficient of friction, and thermal stability, depending on its composition and stoichiometry. Titanium nitride (TiN) was the very first PVD coating used in industry, introduced initially for cutting tools.[42]

There are different PVD coating techniques, the most used in industry being "cathodic arc" and "magnetron sputtering." In both processes, the film's metallic fraction is evaporated from a "target," whose composition has a metal purity of approximately 99.999% or the composition of the alloy. Process gases are nitrogen and argon with 99.999% purity, and methane with 99.95%. Nitrogen and methane are gas carriers for the nitride or carbide coating type. The process takes place in a high-vacuum chamber, reaching levels up to 10^{-6} torr.

Figure 25 schematically shows the cathodic arc deposition process. Once the parts are properly heated under vacuum, the anode/cathode assembly in the target region receives an electric discharge that evaporates the metal atoms. Simultaneously, the reactive gas (N_2 or CH_4) is injected into the chamber in the presence of a plasma atmosphere, which will provide the non-metallic element. The evaporated atoms and the gases in the atmosphere are ionized, assuming a positive (+) charge, accelerated, and collide with the surface of the part to be coated, which

is under a negative voltage, called "bias," which attracts the (+) ions present in the atmosphere and promotes condensation and coating formation.[42-45] Figure 26 shows schematically the mass transport and reactions occurring during the formation of a TiN PVD layer.

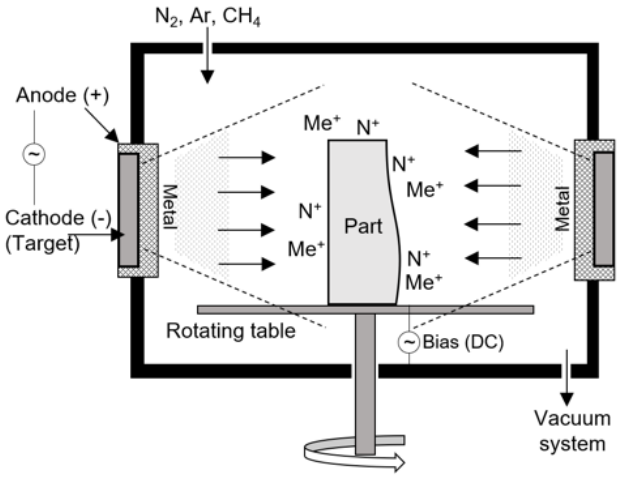

Figure 25: Cathodic arc PVD deposition process.
Source: Elaborated by the authors.

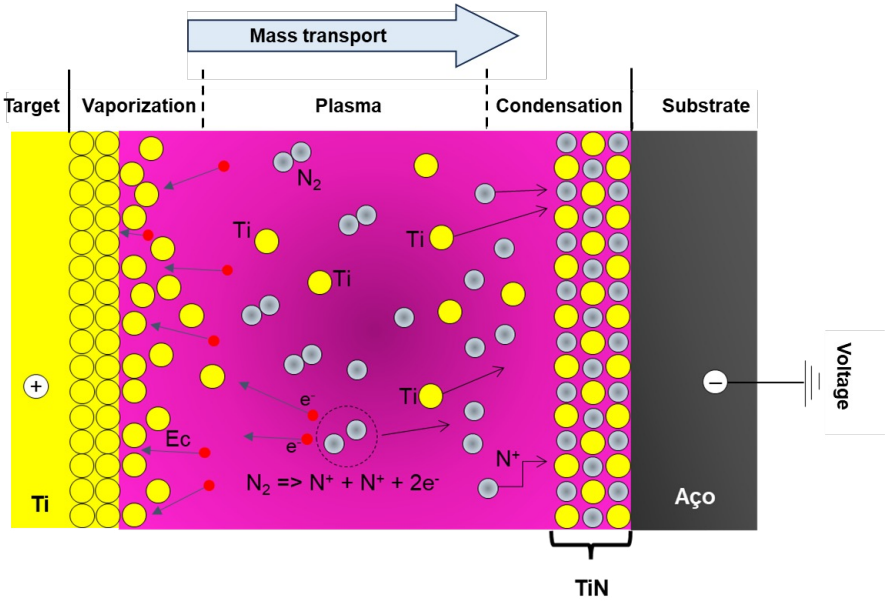

Figure 26: Mass transport during Arc/PVD deposition process.
Source: Elaborated by the authors.

PVD layers generally have thicknesses between 1.0 and 6.0 µm, specified according to the layer type and application. Table 2 shows the most commonly used PVD layers in industry, and Fig. 27 shows tools coated with TiN and CrAlN. The process can apply a single layer, "monolayer," or several layers of different compounds, "multilayer." The use of multilayers aims to improve tribological properties, particularly against wear and corrosion, and adhesion of the layer to the substrate.[46] Figure 28 shows (a) the cross-section of a TiN monolayer and (b) a multilayer consisting of Ti-TiN deposited alternately. Under both conditions, the growth of the TiN layer with a typical columnar structure is clearly observed. In this case, the use of this multilayer system promoted a 22% increase in adhesion.[46]

Table 2: Characteristics of PVD coating films.

Composition	Hardness HV	Coefficient of friction	Thermal stability (oC)	Color
TiN	2,200	*0.40*	*600*	Gold-yellow
CrN	1,800	*0.40*	*700*	Silver-gray
TiAlN	3,300	*0.50*	*900*	Violet-gray
CrAlN	3,200	*0.40*	*1,000*	Bright gray

Source: Courtesy of HTS Tecnologia em Revestimentos Ltda.

TiN CrAlN

Figure 27: Parts after arc-PVD coating.
Source: Courtesy of HTS Tecnologia em Revestimentos Ltda.

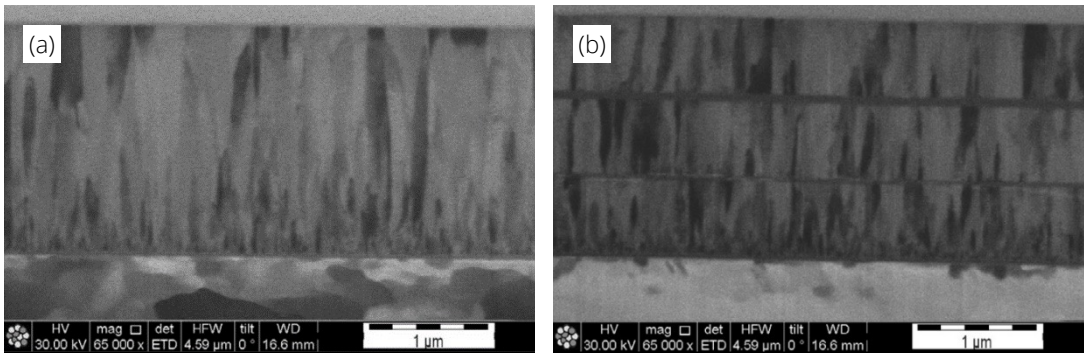

Figure 28: TiN monolayer (a) and Ti/TiN multilayer (b).[46]
Source: Adapted from Ali et al.[46]

Recent developments in coatings technology are nitride layers based on high-entropy alloys (HEAs) with improved properties: high hardness, wear resistance, oxidation resistance, and thermal stability. The concept of high-entropy is the use of a multicomponent alloy system with at least five components. This optimization of properties is due to the high entropy of mixing, which increases with an increase in the number of elements in the composition.[47] Figure 29 shows a comparison between the regular TiN layer and an HEA alloy, which is based on (VTiMoCu) nitride.

PVD coating technology is widely used in tool steels to improve in-service performance. PVD layers have high hardness and a low coefficient of friction, properties that are fundamental for improving cutting capacity, cold work forming capacity, and shear cutting operations. Figure 30 shows the results of a pin-to-disc wear test for AISI M2 high-speed steel with and without a PVD coating, using titanium carbonitride (TiCN), in which the mass loss due to wear decreases significantly in the presence of the coating.[48]

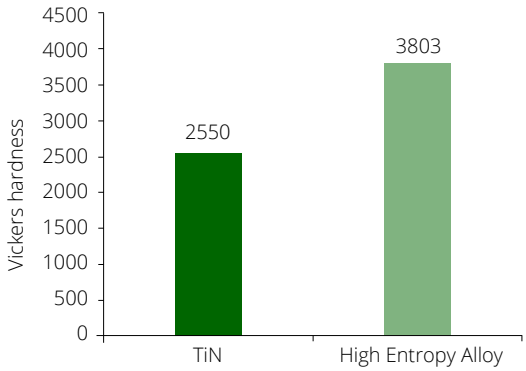

Figure 29: Nanoindentation hardness test for TiN and a (VTiMoCu) nitride HEA. Test load 10 mN.
Source: Courtesy of HTS Tecnologia em Revestimentos Ltda – unpublished research.

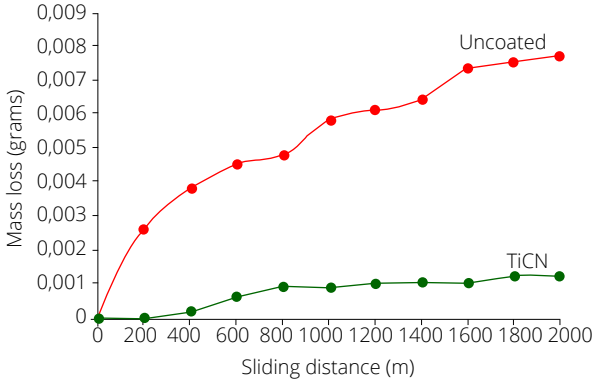

Figure 30: Mass loss in a pin-to-disc wear test, under a 38.6 N force, for a TiCN-coated high-speed steel AISI M2.[48]
Source: Adapted from Bressan et al.[48]

The surface quality of parts intended for PVD coating plays an important role in the final performance, as it is a fundamental factor in the adhesion of the coating to the substrate and, therefore, the service life of the coated parts.[49] Thus, surface quality must be conditioned at least by fine grinding and, at best, by polishing to control roughness. High roughness reduces the actual contact area, making the system more prone to abrasive wear or fatigue. High roughness significantly affects the distribution of residual stresses at the coating/substrate interface and can compromise layer adhesion.[50,51]

Surface cleaning is also crucial for adhesion because any contaminants present on the parts' surface, inside thin gaps/holes, or welding-repaired areas impair proper layer adhesion during the process or in service. Despite careful prior cleaning in ultrasound systems, the PVD process involves a long cleaning step, using ion sputtering under plasma at vacuum levels close to 10^{-5} torr, requiring the use of diffusion or turbomolecular vacuum pumps. These steps involve degassing, ion sputtering, removal of surface residues, oxidation removal by hydrogen reduction, and surface activation. Preheating and cleaning can account for up to two-thirds of the total processing time. Figure 31 shows loss of adhesion along a welding zone (arrows) not informed of and not detected before the PVD process.

Figure 31: Loss of adhesion of arc-PVD layer on the welding area just after the process finishes.
Source: Courtesy of HTS Tecnologia em Revestimentos Ltda.

DUPLEX SURFACE TREATMENT

HTGN and LTPN

A Duplex surface Treatment consisting of a combination of an HTGN, which hardens a thick layer of austenite to 300 to 400 HV, with an LTPN treatment carried out in a DC plasma reactor, which forms a thin, super-hard, γ_N expanded austenite layer. The thick, medium-hardened intermediate gas nitrided layer provides mechanical support to a very hard expanded austenite layer, as schematically shown in Fig. 32.[52] The mechanical support given by the intermediate layer results in much better wear resistance in demanding applications, where extremely high contact pressures stress the bi-layer hardened surface.

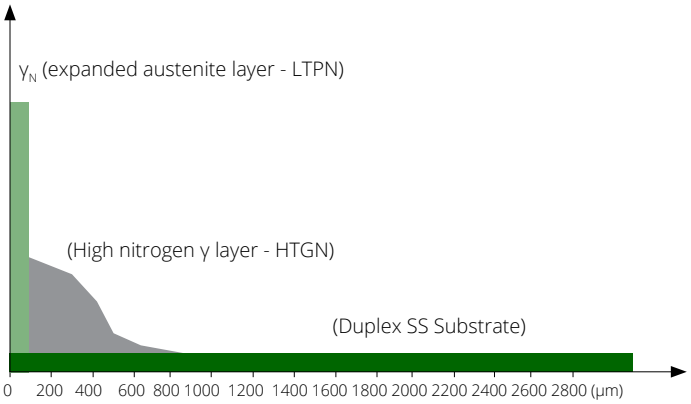

Figure 32: Schematics showing the thick HTGN reinforcing layer, which gives mechanical support to a very thin, super-hard, expanded austenite layer (γ_N).[52]

Source: Adapted from Mesa et al.[53]

Mesa et al.[53] studied the cavitation erosion resistance of a UNS 31803 Duplex Stainless Steel under different conditions, including as received, HTGN, and DSS HTGN + LTPN. Figure 33 shows the surface microstructure with a fully ASS case obtained by HTGN and expanded austenite on the outermost surface obtained after LTPN. For cavitation tests, ASS stainless steel UNS 30403 was used for comparison with the as-received non-hardened ASS matrix and after LTPN. For DSS UNS 31803, Fig. 34 shows much better behavior under cavitation erosion of the DSS HTGN + LTPN condition compared to the as-received and HTGN conditions. UNS 30403 ASS shows better performance compared to UNS 31803 DSS for the as-received non-treated condition, increasing performance with LTPN. The increase in cavitation performance solely by HTGN of austenite is evident when comparing the non-hardened ASS matrix of UNS 30403 ASS with the UNS 31803 DSS fully ASS case hardened by HTGN.

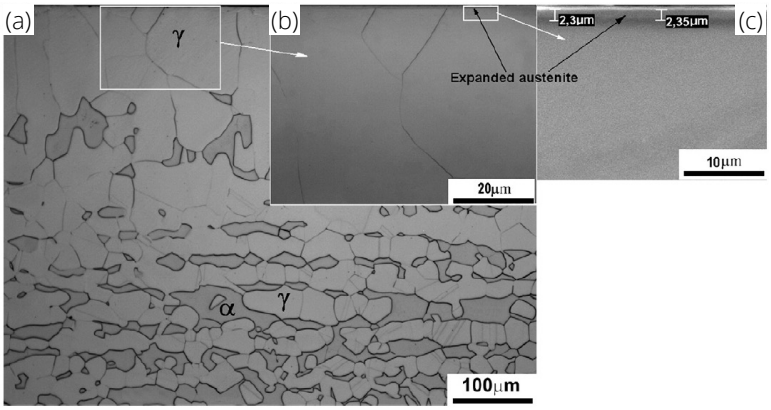

Figure 33: Optical cross-section of the DSS-treated (HTGN+LTPN) UNS S31803 stainless steel. (a) α+γ microstructure in the core and a 100 µm thick fully ASS microstructure at the surface, (b) fully ASS layer, and (c) expanded austenite layer.[53]

Source: Adapted from Mesa et al.[53]

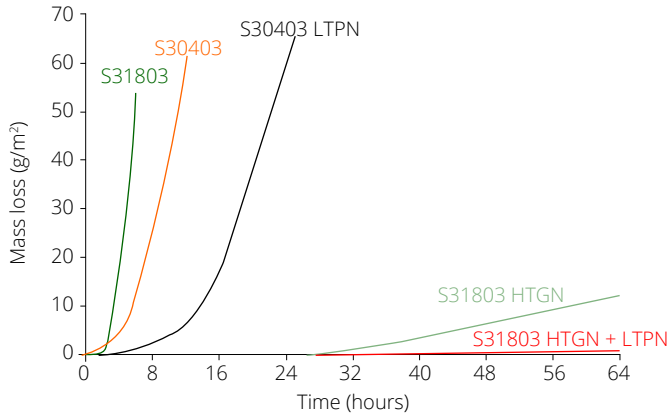

Figure 34: Cavitation erosion wear rates of ASS UNS 30403 ASS and DSS UNS 31803 DSS.[53]
Source: Adapted from Mesa et al.[53]

Plasma nitriding and PVD

Combined nitriding and PVD coating, called "Duplex Surface Treatment," has proved an important option to enhance the lifetime of tool steel tools. It is well known that a DSS treatment can significantly increase the wear performance due to the promoted load-carrying capacity, increased by the NC, and thus increasing the adhesion of the hard ceramic PVD coating layer.

Studying DSS treatment for hot work tool steel type AISI H13, Adonias et al.[54,55] showed that TiN coating adhesion is strongly dependent on the mechanical properties of the nitrided layer close to the interface. The adhesion condition was found to increase when the relation H/E and the amount of elastic recovery of the NC are close to those of the TiN coating.

Hardness and depth of the NC and TiN layer are shown in Fig. 35. For all nitriding conditions, the maximum hardness was greater than 1000 HV0.005. NC depth increases with nitriding time due to nitrogen diffusion. Hardening of the surface after plasma nitriding is essential to guarantee a good load support effect for the TiN coating. The TiN layer average thickness was 6.55 ± 0.21 µm, and the average hardness was 2217.5 ± 47.4 HV0.005.

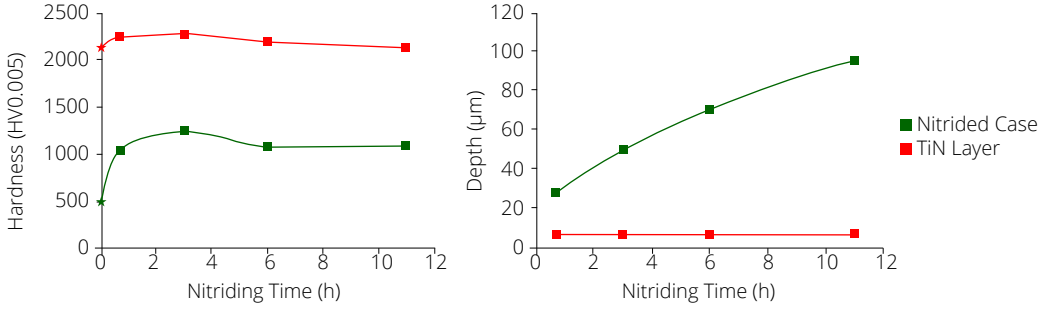

Figure 35: TiN coating and NC hardness vs. nitriding time, and nitriding case depth and TiN thickness.
Source: Adapted from Franco Jr et al.[54]

Rockwell "C" indentation tests, using the Daimler method, showed that failure occurs primarily through the formation of radial Hertz cracks in the form of circles around the indentation area, which define the critical cracking load *Lc1*.[56,57] With increasing indentation load, the progression of cracks initiates delamination, promoting the removal of the coating and exposure of the substrate, defining the critical delamination load *Lc2*, related to the loss of the load-bearing capacity effect of the substrate. Figure 36 shows the values of the critical loads *Lc1* and *Lc2* for AISI H13 steel nitrided for different times in a gas mixture with 5% N_2, without the presence of the compound layer. Increasing the nitriding time promotes an increase in the critical loads *Lc1* and *Lc2*, due to the increase in nitriding depth and consequently the increase in the load-bearing effect of this case in relation to the TiN coating layer.

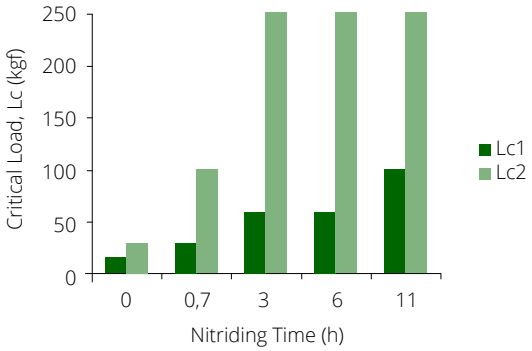

Figure 36: Critical loads for cracking (*Lc1*) and delamination (*Lc2*) during a Daimler adhesion test as a function of the nitriding time.
Source: Adapted from Franco Jr et al.[54]

Elastic recovery, defined by the ratio between hardness and the modulus of elasticity, H/E, determined by depth-sensing nanoindentation tests, is an important parameter for comparing the compatibility between the properties of the nitrided layer and those of the PVD coating. Figure 37 shows that nitriding is efficient in obtaining an H/E ratio close to that of the TiN coating, demonstrating the important role of the nitrided substrate layer beneath the coating in increasing adhesion by optimizing the elastic properties at the interface.

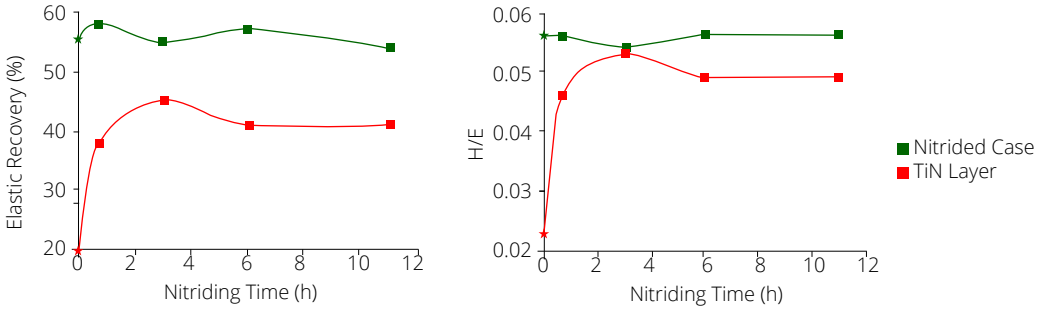

Figure 37: Elastic recovery and H/E ratio of the TiN coating and the NC as a function of the nitriding time.
Source: Adapted from Franco Jr et al.[54]

As previously mentioned, one of the main advantages of the plasma nitriding process is the control of NC microstructure due to the possibility of close control of nitriding potential via the nitrogen content in the gas mixture (Fig. 16). For duplex treatment, the presence of the compound layer proved to be deleterious for TiN PVD layer adhesion. Figure 38 compares the performance of pre-nitrided surfaces with and without compound layer formation. The results show a decrease in adhesion properties when nitriding is performed with compound layer formation.

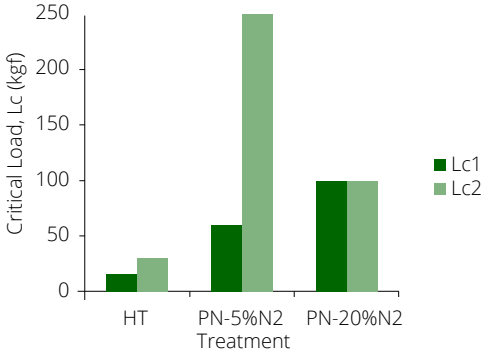

Figure 38: Critical load for cracking (Lc1) and delamination (Lc2) in pre-nitrided samples under different nitrogen contents in the gas mixture.
Source: Adapted from Franco Jr et al.

In this case, the results cannot be explained solely by the load-bearing effect, considering the surface hardening effect obtained by nitriding with 20% vol. N_2. Microstructural aspects related to the phase transformation of the compound layer during the PVD process affect adhesion. Figure 39 shows the microstructure of the DSS surface; nitrided layer at 520 °C/6 h with 20%vol. N_2. After PVD, it is observed that the compound layer transforms, assuming the morphology of a "black layer" (BL) located between the TiN coating and the diffusion zone of the NC. Sun and Bell[4] and Dingremont[5] suggest that this layer consists of ferrite and nitrides, formed as a product of the phase transformation of the compound layer as a result of exposure to temperature and time during the PVD process.

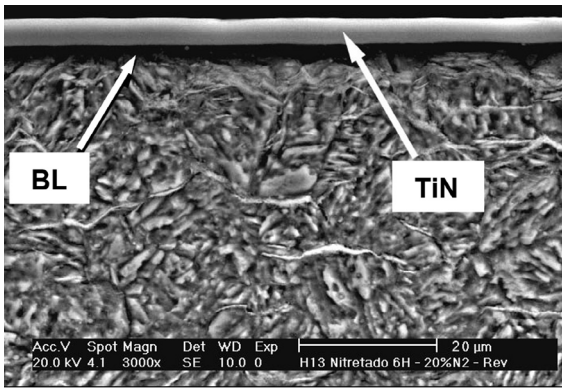

Figure 39: DSS surface, plasma nitrided at 520 °C/6 h/20%N2:80%H2, after TiN-PVD coating.
Source: Adapted from Franco Jr et al.55

Figure 40 also shows the transverse hardness and H/E profiles of the NC with a compound layer, before and after PVD coating. It can be seen that before coating, the hardness reaches a maximum value of 1052 HV0.005, with an H/E ratio close to 0.06, therefore close to the H/E of TiN. These mechanical properties would predict good adhesion performance, as they are close to those of the coating. However, the phase transformation in the compound layer that occurs during PVD deteriorates the mechanical properties at the interface, locally decreasing the hardness up to 910 HV0.005, reducing the H/E ratio up to 0.049, accounting for the poor performance of these Duplex surfaces compared to the nitrided surface without a compound layer. In this case, the load-bearing effect for TiN is reduced at the interface, and the tribological properties are deteriorated.

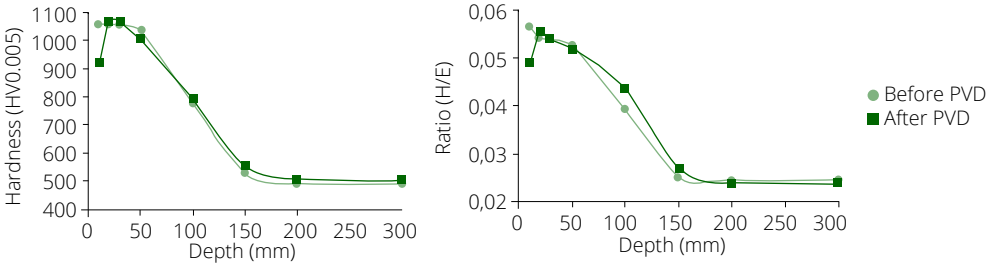

Figure 40: Variation in hardness and H/E ratio of the nitrided surface with a compound layer, 20% vol. N2, before and after the TiN-PVD coating.
Source: Adapted from Franco Jr et al.[55]

SEM evaluations of the HRC indentations for adhesion tests clearly demonstrate the difference in adhesion behavior of the NC with and without the compound layer. Figure 41a shows the load-bearing effect achieved by nitriding without a compound layer, where only cracks are observed in the coating and substrate without delamination. Figure 41b demonstrates the deterioration caused by the presence of the compound layer after pre-nitriding, with the formation of deeper cracks in the coating, at the interface, and on the substrate, with intense coating loss due to delamination. As pointed out, the reason for this differential adhesion behavior is related to the mechanical properties of the substrate in the interface region with TiN.

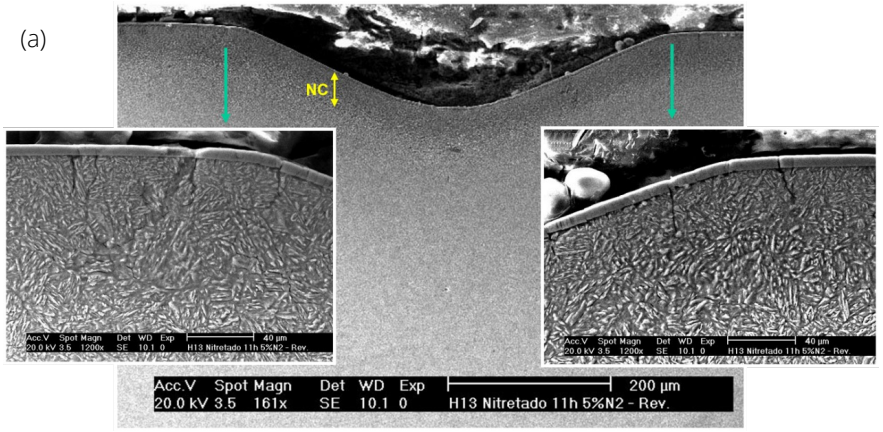

Without a compound layer. 5%N_2:95%H_2.

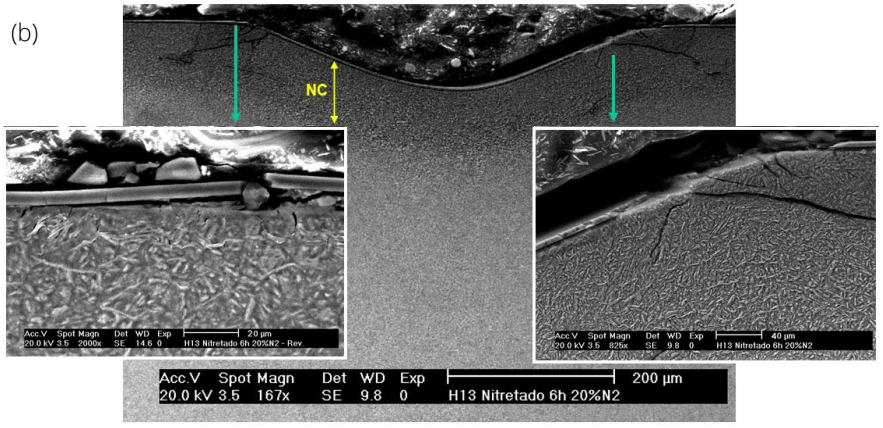

With a compound layer. 20%N_2:80%H_2.

Figure 41: Cross-section of the HRC indentation area for DSS-treated AISI H13 tool steel.
Source: Adapted from Franco Jr et al.[55]

PERSPECTIVES AND OUTLOOKS

Environmental issues are undoubtedly one of the most important factors driving the growth of vacuum heat and surface treatment processes in the coming decades. Coupled with this is the increasing need for advanced materials with superior performance, energy efficiency, and sustainability requirements in manufacturing processes. In other words, factors driven by innovations in materials science and the expansion of its applications in high-tech sectors. The near future indicates a set of factors in the consolidation of the integration of new technologies, enhancing process efficiency and quality control. Emerging technologies, such as "Industry 4.0," "Internet of Things," and "Artificial Intelligence," are revolutionizing furnace operations in terms of process time, maintenance criteria, efficiency, and reliability.

The future scenario indicates the development and consolidation of (i) vacuum heat treatment furnaces for special steels and alloys equipped with superior automation, control, and cooling capacity, (ii) low-temperature plasma diffusion processes combined with subsequent oxidation or deposition surface treatments, and (iii) increasing use of new PVD technologies such as magnetron sputtering, high-power impulse magnetron sputtering, reactive sputtering and co-sputtering.

CONFLICT OF INTEREST

Nothing to declare.

AUTHOR CONTRIBUTIONS

Conceptualization: Pinedo CE and Tschiptschin AP; **Writing - First draft:** Pinedo CE and Tschiptschin AP; **Writing - Proofreading & Editing:** Pinedo CE; **Final approval:** Pinedo CE

DECLARATION OF USE OF INTELLIGENCE ARTIFICIAL TOOLS

The authors declare that no artificial intelligence tools were used in the preparation, writing, data analysis, or review of this manuscript.

AVAILABILITY OF DATA AND MATERIALS

Not applicable.

FUNDING

Not applicable.

ACKNOWLEDGEMENTS

Not applicable.

REFERENCES

1. Pinedo CE. Fundamentos da nitretação sob plasma para o tratamento superficial de aços e ligas especiais. Anais da II Conferência Brasileira sobre Temas de Tratamento Térmico; 2004; Atibaia, São Paulo, Brasil.
2. Holmberg K, Matthews A. Coatings tribology: properties, techniques and applications in surface engineering. Oxford: Elsevier Science B.V.; 1994.
3. ISO 14000 Family: International Standards on Environmental Management. Available from: https://www.iso.org/standards/popular/iso-14000-family
4. Liščić B. Heat transfer control during quenching. Mater Manuf Process. 2009;24(7-8):879-86. https://doi.org/10.1080/10426910902917694
5. Totten GE. Steel heat treatment handbook. 2nd ed. Boca Raton: CRC Press; 2007.
6. Ruffle TW, Byrnes ER. Quenching in vacuum furnaces. Heat Treat Met. 1979;4:81-7. In: Handbook of residual stress. Chicago: ASM International; 2002.
7. Nichols HP. Standardizing H-13 die cast heat treatment. Proceedings of Conference: International European Conference on Tooling Materials, New Materials Processes Experiences for Tooling; 1992 Sep 7-9; Interlaken, Switzerland.
8. North American Die Casting Association (NADCA). Premium and Superior Quality H13 Steel and Heat Treatment Acceptance Criteria for Pressure Die Casting Dies. NADCA Technical Report nº 207; 2003.
9. Wingens T. Maximizing quenching and cooling in vacuum heat treating. Proceedings of the 28th ASM Heat Treating Society Conference; 2015 Oct 20-22; Detroit, Michigan, USA.

10. Borgioli F, Adachi S, Lindner T. Advances in low-temperature nitriding and carburizing of stainless steels and metallic materials: formation and properties. Metals (Basel). 2024;14:1179. https://doi.org/10.3390/met14101179

11. Santos J, Garzón CM, Tschiptschin AP. Improvement of the cavitation erosion resistance of an AISI 304L austenitic stainless steel by high temperature gas nitriding. Mater Sci Eng A. 2004;382(1-2):378-86. https://doi.org/10.1016/j.msea.2004.05.003

12. Mingolo N, Tschiptschin AP, Pinedo CE. On the formation of expanded austenite during plasma nitriding of an AISI 316L austenitic stainless steel. Surf Coat Technol. 2006;201(7):4215-8. https://doi.org/10.1016/j.surfcoat.2006.08.060

13. Pinedo CE, Tschiptschin AP. Low temperature nitriding, nitrocarburizing and carburizing of AISI 316L austenitic stainless steel. Int Heat Treat Surf Eng. 2011;(5):73-7. https://doi.org/10.1179/174951411X13051201040703

14. Fontanna MG. Corrosion engineering. 3rd ed. New York: McGraw Hill Book Company; 1987.

15. France WD, Greene ND. Predicting the Intergranular Corrosion of Austenitic Stainless Steels. 21st NACE Conference; 1965 Mar 15-19; St. Louis, MO.

16. Garzon CM, Tschiptschin AP. EBSD texture analysis of a high temperature gas nitrided duplex stainless steel. Mater Sci Eng A. 2006;441:230-8. https://doi.org/10.1016/j.msea.2006.08.018

17. Speidel MO. HNS 2003 high nitrogen steels. Zürich: VDF Hochschulverlag; 2003.

18. Garzon CM, Tschiptschin AP. New high temperature gas nitriding cycle that enhances the wear resistance of duplex stainless steels. J Mater Sci Lett. 2004;3(9):7101-5. https://doi.org/10.1023/B:JMSC.0000047559.15644.97

19. Collins SR, Williams PC, Marx SV, Heuer A, Ernst F, Kahn H. Low-temperature carburization of austenitic stainless steels. ASM Handbook. Volume 4D, Heat treating of irons and steels. Chicago: ASM International; 2014.

20. Kolster BH. Verschleiß- und korrosionsfeste Schichten auf austenitischen Stählen. Düsseldorf: VDI-Berichte. 1983;506:107-13.

21. Ichii K, Fujimura K, Takase T. Structure of the ion-nitrided layer of 18-8 stainless steel. Tech Rep Kansai Univ. 1986;27:135-44. https://doi.org/10.1201/9780367814151-3

22. Pinedo CE, Tschiptschin AP. Low temperature nitriding, nitrocarburizing and carburizing of AISI 316L austenitic stainless steel. Int Heat Treat Surf Eng. 2011;5:73-7. https://doi.org/10.1179/174951411X13051201040703

23. Borgioli F. From austenitic stainless steel to expanded austenite-S phase: formation, characteristics and properties of an elusive metastable phase. Metals (Basel). 2020;10(2):187. https://doi.org/10.3390/met10020187

24. Edenhofer B. Physical and metallurgical aspects of ionitriding. Heat Treat Met. 1974;1(1).

25. Edenhofer B. Physical and metallurgical aspects of ionitriding. Heat Treat Met. 1974;1(2).

26. Thelning KE. Case hardening. In: Steel and its heat treatment. New York: McGraw-Hill; 1975.

27. Strämke S, Dressler S. Plasma nitriding using pulsation – a surface treatment without pollution. Pittsburgh: Ind Heat; 1985.

28. Hüchel U, Dressler S. Pulsed plasma nitriding for the automotive industry production experience. In: Proc. Conf., Heat Treatment Conference; 1994 Apr; Chicago, Illinois. ASM International.

29. Pinedo CE. Nitretação por plasma. Anais do I Seminário Internacional de Engenharia de Superfície. Núcleo de Pesquisas Tecnológicas da Universidade de Mogi das Cruzes; 1995.

30. Verma R, Podob M. Plasma nitriding: state-of-the-art. Pittsburgh: Ind Heat; 1985.

31. Jones CK. Ion nitriding. In: Heat treatment '73: Proceedings of the conference. London: The Metals Society; 1973. p. 71 7.

32. Spalvins T. Advantages and directions of ion nitriding/nitrocarburizing. In: Ion Nitriding and Ion Carburizing. Proceedings of the ASM 2nd International Conference on Ion Nitriding/Carburizing; 1989.

33. Elwart J, Hunger R. Plasma (ion) nitriding and nitrocarburizing of steels. ASM Handbook. Steel heat treating fundamentals and processes. Volume 4A. Chicago: ASM International; 2013.

34. Czerwieca T, Michela H, Bergmann E. Low-pressure, high-density plasma nitriding: mechanisms, technology and results. Surface Coatings Technol. 1998;108/109:182-90. https://doi.org/10.1016/S0257-8972(98)00555-6

35. Hassouba MA, Mehanna EA. Electrical characteristics of (N2-H2) gas mixture DC glow discharge. Int J Phys Sci. 2009;4(11):713-21.

36. Rizk AS, McCulloch DJ. Plasma nitriding of Inconel 625. Surf Technol. 1979;9:303-15. https://doi.org/10.1016/0376-4583(79)90061-X

37. Leroy C, Czerwiec T, Gabet C, et al. Plasma assisted nitriding of Inconel 690. Surf Coatings Technol. 2001;142:241-7. https://doi.org/10.1016/S0257-8972(01)01243-9

38. Tschiptschin AP, Nishikawa AS, Varela LB, Pinedo CE. Thermal stability of expanded austenite formed on a DC plasma nitrided 316L austenitic stainless steel. Thin Solid Films. 2017;644:156-65. https://doi.org/10.1016/j.tsf.2017.06.065

39. Pinedo CE, Tschiptschin AP. Low temperature nitriding, nitrocarburizing and carburizing of AISI 316L austenitic stainless steel. Int Heat Treat Surf Eng. 2011;5:73-7. https://doi.org/10.1179/174951411X13051201040703

40. Makishi T, Nakata K. Surface hardening of nickel alloys by means of plasma nitriding. Metall Mater Trans A Phys Metall Mater Sci. 2004;35A:227-38. https://doi.org/10.1007/s11661-004-0123-7

41. Varela LB, Ordoñez MFC, Pinedo CE, Tschiptschin AP. Micro-abrasive wear study of a low-temperature plasma nitrided Inconel 625 superalloy. Tribology Mater Surf Interfaces. 2021;16(2):119-29. https://doi.org/10.1080/17515831.2021.1898899

42. Sanders DM, Boercker DB, Falabella S. Coating technology based on the vacuum arc – a review. IEEE Trans Plasma Sci. 1990;18:883-94. https://doi.org/10.1109/27.61499

43. Baptista A, Silva F, Porteiro J, Míguez J, Pinto G. Sputtering physical vapour deposition (PVD) coatings: a critical review on process improvement and market trend demands. Coatings. 2018;8:402-24. https://doi.org/10.3390/coatings8110402

44. Mattox DM. Arc vapor deposition. In: Handbook of physical vapor deposition (PVD) processing. 2nd ed. Boston: William Andrew; 2010.

45. Koskinen J. Cathodic-arc and thermal-evaporation deposition. In: Hashmi MSJ, Batalha GF, Van Tyne CJ, Yilbas BS, editors. Comprehensive materials processing. Amsterdam: Elsevier; 2014. p. 3-5. https://doi.org/10.1016/B978-0-08-096532-1.00409-X

46. Ali R, Sebastiani M, Bemporad E. Influence of Ti-TiN multilayer PVD-coatings design on residual stresses and adhesion. Mater Des. 2015;75:47-56. https://doi.org/10.1016/j.matdes.2015.03.007

47. Novikov V, Stepanov N, Zherebtsov S, Salishchev G. Structure and properties of high-entropy nitride coatings. Metals. 2022;12:847. https://doi.org/10.3390/met12050847

48. Bressan JD, Hesse R, Silva Jr EM. Abrasive wear behavior of high speed steel and hard metal coated with TiAlN and TiCN. Wear. 2001;250:561-8. https://doi.org/10.1016/S0043-1648(01)00638-X

49. Tönshoff HK, Karpuschewski B, Mohlfeld A, Seegers H. Influence of subsurface properties on the adhesion strength of sputtered hard coatings. Surf Coat Technol. 1999;116-119:524-529. https://doi.org/10.1016/S0257-8972(99)00226-1

50. Holmberg K, Matthews A, Ronkainen H. Coatings tribology – contact mechanisms and surface design. Tribol Int. 1998;31(1-3):107-120. https://doi.org/10.1016/S0301-679X(98)00013-9

51. Matthews A, Leyland A, Holmberg K, Ronkainen H. Design aspects for advanced tribological surface coatings. Surf Coat Technol. 1998;100-101:1-6. https://doi.org/10.1016/S0257-8972(97)00578-1

52. Tschiptschin AP. Duplex coatings. In: Wang Q Jane, Chung Yip-Wah, organizadores. Encyclopedia of tribology. Munich: Springer US; Volume 2; 2013.

53. Mesa DH, Pinedo CE, Tschiptschin AP. Improvement of the cavitation erosion resistance of UNS S31803 stainless steel by duplex treatment. Surf Coat Technol. 2010;205:1552-6. https://doi.org/10.1016/j.surfcoat.2010.10.014

54. Franco Jr AR, Pinedo CE, Tschiptschin AP. Influence of the plasma pre-nitriding surface treatment on wear and adhesion of PVD/Tin coating for the hot work tool steel AISI H13. 7th International Tooling Conference "Tooling materials and their applications from research to market"; 2-5 May 2006; Interlaken, Switzerland.

55. Franco Jr. AR, Pinedo CE, Tschiptschin AP. Utilização da nitretação sob plasma como pré-tratamento ao revestimento TiN-PVD na geração de superfícies dúplex no aço AISI H13. 5o Encontro da Cadeia de Ferramentas, Moldes e Matrizes da ABM; 2007.

56. Souza RM, Sinatora A, Mustoe GGW, Moore JJ. Numerical and experimental study of the circular cracks observed at the contact edges of the indentation of coated systems with soft substrates. Wear. 2001;251:1337-46. https://doi.org/10.1016/S0043-1648(01)00778-5

57. Hedenqvist P, Olsson M, Söderberg S. Failure analysis of TiN-coated high speed steel: in situ scratch testing in the scanning electron microscopy. Surf Coat Technol. 1990;41:31-49. https://doi.org/10.1016/0257-8972(90)90128-Y